Excited Charge Separation in a π-Interacting Phenothiazine-ZincPorphyrin-Fullerene Donor-Acceptor Conjugate

B. Yadagiri,[a,b] Ram Ratan Kaswan,[c] Jairam Tagare,[a] Vinay Kumar,[a,b] Manne Naga Rajesh,[a,b] Surya Prakash Singh[a,b*] Paul A. Karr,[d] Francis D'Souza,[c,*] Lingamallu Giribabu[a,b*]

[a]Department of Polymers and Functional Materials, CSIR-Indian Institute of Chemical Technology, Uppalroad, Tarnaka, Hyderabad-500007, India.

[b]Academy of Scientific and Innovative Research, CSIR-IICT.

[c]Department of Chemistry, University of North Texas, 1155 Union Circle, #305070, Denton, TX 76203-5017, USA.

[d]Department of Physical Sciences and Mathematics, Wayne State College, 111 Main Street, Wayne, Nebraska 68787, USA

E-mail: spsingh@iict.res.in, francis.dsouza@unt.edu, giribabu@iict.res.in

Abstract

We have designed, synthesized, and characterized a donor-acceptor molecular system, **SPS-PPY-C_{60}**, that consists of a π-interacting phenothiazine linked porphyrin as a donor and sensitizer, and fullerene as an acceptor to seek charge separation upon photoexcitation. The optical absorption spectrum revealed red-shifted Soret and Q-bands of porphyrin due to the presence of two ethynyl bridges carrying substituents. The redox properties suggested that the phenothiazine-porphyrin part of the molecule is easier to oxidize and the fullerene part is easier to reduce. DFT calculations supported the redox properties wherein the electron density of the highest molecular orbital (HOMO) was distributed over the donor phenothiazine-porphyrin entity while the lowest unoccupied molecular orbital (LUMO) was distributed on fullerene acceptor. The steady-state emission spectrum, when excited either at porphyrin Soret or visible band absorption maxima, revealed quenched emission both in non-polar and polar solvents suggesting the occurrence of excited state events. Finally, femtosecond transient absorption spectral studies were performed to witness the charge separation by utilizing solvents of different polarities. The transient data was further analyzed by GloTarAn by fitting the data with appropriate models to describe photochemical events. From this, the average lifetime of the charge-separated state calculated was found to be 169 ps in benzonitrile, 319 ps in dichlorobenzene, and 1.7 ns in toluene for Soret band excitation, and ~320 ps for Q-band excitation in benzonitrile was obtained.

Introduction

The transformation of sun light into different forms of energy by following natural or artificial photosynthesis path is an attractive and fascinating topic that has inspired researchers in physics, chemistry, and biology.[1-7] Photosynthesis exemplifies a remarkable model that has inspired the design of numerous complex assemblies to translate light energy into chemical potential. A great variety of Donor-Acceptor (D-A) systems have been reported in the literature to understand the photoinduced events and the underlying mechanisms.[8-15]

The photodynamics of D-A systems revealing charge-separated species of appreciable lifetimes is not only useful for understanding the initial events of photosynthesis but also useful in the design of efficient materials for optoelectronic applications.[16-17] Quite a few molecular or supramolecular systems such as dyads, triads, tetrads, etc., have been elegantly designed and studied to witness long-lived charge-separation mimicking "antenna-reaction center" events of photosynthesis.[18-22] Of various scaffolds used for building D-A systems, porphyrins, structurally close to the natural photosynthetic chlorophyll pigment and due to well-established synthetic protocols, have conquered this area of research. Many groups including our groups have reported multi-modular systems by introducing secondary donors/acceptors on the porphyrin macrocycle to achieve sequential electron and hole transfer resulting in the generation of the long-lived charge-separated species.[9,23-30] For instance, Tian and co-workers have developed zinc porphyrin – viologen (ZnP-V) nanoparticles in an aqueous solution that showed a charge separation (CS) state lifetime of up to 4.3 ms.[21] This can be recognized as charge hopping induced by aggregation or distance modification between the donor and acceptor induced by electronic interaction.[22] D'Souza and co-workers[23] have developed bis-benzimidazole-fused porphyrin hetero and homo dimmers in which the axial position of zinc porphyrin coordinated by phenyl imidazole functionalized C_{60}. The split in the Soret band suggested the presence of excitonic coupling while transient absorption studies suggested that the lifetime of the final charge-separated state was in the 30–40μs range.[22] Poddutoori and co-workers have reported a triad system in which a secondary donor bis-triphenylamino-boron-dipyrromethane (TPA_2-BDP) was covalently connected to the axial position of Al(III) porphyrin ($AlPorF_3$), a primary donor and an acceptor pyridine appended naphthalenediimide (NDI) at another axial position and observed charge separated state of $(TAP_2\text{-BDP})^{\bullet+}$-AlP or F_3-$NDI^{\bullet-}$.[9] Zhu et al. developed a two triads featuring

fulleropyrrolidine–perylene tetracarboxylicdiimide–freebase porphyrin (FPP) and its zinc derivative (ZnFPP) for organic solar cells with device efficiency of 0.35%.[10] Absorption and redox properties of these triads suggested that there exist ground state electronic interactions in these triads and emission properties indicate that there was an efficient photoinduced electron transfer (PET) from porphyrin to C_{60}.[29] In another study, Giribabu et al., have reported a triad system in which phenothiazine is primary donor, porphyrin is the secondary donor and thiophene cyano acrylic acid is an acceptor for dye-sensitized solar cell application in which the device efficiency was >10%.[26] Femtosecond transient absorption studies suggested that the hole formed on porphyrin after the injection of an electron to TiO_2 conduction band migrated to primary donor phenothiazine and a long-lived charge-separated state formed.[25]

In continuation of our efforts towards the design of porphyrin-based donor-acceptor systems, in the present study, a π-interacting phenothiazine was linked to a zinc porphyrin at its meso position using a triple bond and a fulleropyrrolidine acceptor through a bisthiophene spacer that was tethered through a triple bond at the opposite side of the meso position (**SPS-PPY-C_{60},** see Chart 1 for structure). Phenothiazine possesses a non-planar butterfly conformation, that absorbs in the UV region, exhibiting low oxidation potentials, and possesses a high propensity to form stable radical cations.[31] In contrast, fullerene is a rigid three-dimensional symmetrical shape molecule, requiring very small reorganization energy which is a pre-requisite for efficient electron transfer reactions.[32] Further, the relatively strong absorption in the UV-visible region and multi-step reduction along with its high electron affinity make this unit an attractive candidate in material chemistry, mainly in studying photoinduced electron transfer in donor–acceptor systems[33] and in photovoltaic devices.[34] Key findings on the newly made **SPS-PPY-C_{60}** system are summarized below.

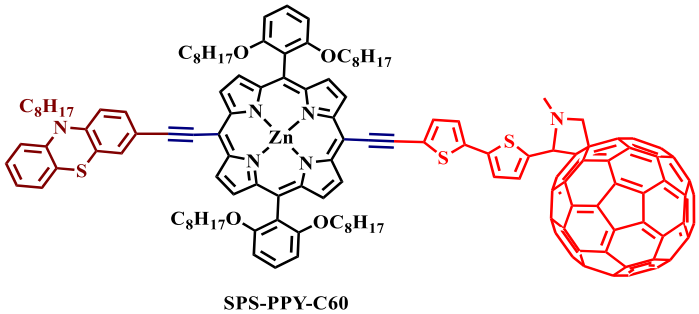

SPS-PPY-C60

Chart 1. Molecular structure of investigated donor-acceptor conjugate, **SPS-PPY-C_{60}**.

2. Experimental Section

2.1 Synthesis

The synthesis of the target compound, **SPS-PPY-C$_{60}$** involved multiple steps, as depicted in Scheme 1. Compounds I, II, III, and IV were synthesized according to the literature procedure.[26,30] The crucial intermediate, compound V was synthesized by adopting the Suzuki coupling reaction between 3-bromo-10-octyl-10H-phenothiazine and compound IV. Similarly, by adopting the Suzuki coupling reaction between V with 5'-bromo-[2,2'-bithiophene]-5-carbaldehyde, the second intermediate VI was obtained. Finally, the desired compound, **SPS-PPY-C$_{60}$** was obtained by following Prato's fulleropyrrolidine synthesis by condensation with fullerene, C_{60} in the presence of sarcosine.[35] Both the donor-acceptor conjugate and control compounds were soluble in many common organic solvents and allowed to be characterized by various spectroscopic techniques (Fig. S1 to S9) and electrochemical methods. The MALDI-MS spectrum of **SPS-PPY-C$_{60}$** showed a peak at m/z = 2016.782 ($C_{139}H_{125}N_6O_4S_3Zn$), which were assigned to their corresponding molecular ion peaks (*see* Fig. S9). Further molecular integrity of **SPS-PPY-C$_{60}$** was confirmed by ^{1}H NMR spectrum (*see* Fig. S8).

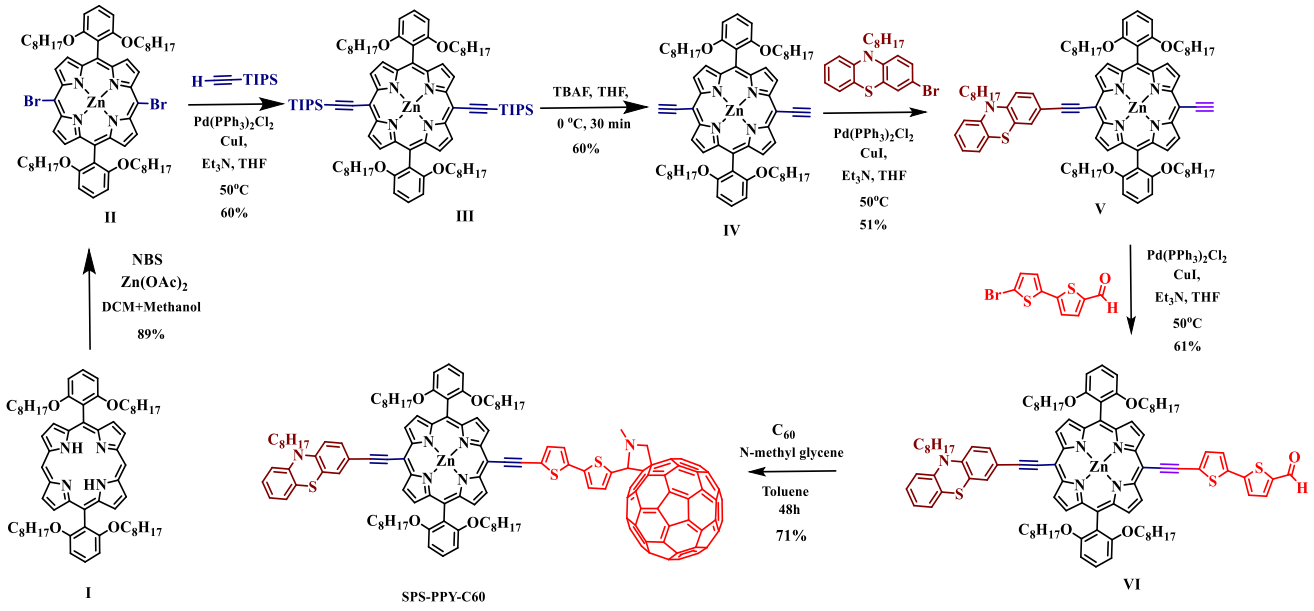

Scheme 1. Synthetic scheme of **SPS-PPY-C$_{60}$**.

The synthetic details of compounds V, VI, and the final compound, **SPS-PPY-C$_{60}$** are given below.

Synthesis of V: A dry round bottom flask (100 mL) was charged with compound IV (2.0 g, 2.05 mmol), phenothiazine (0.75 mL, 3.34 mmol), triethyl amine (12 mL), triphenylphosphine (15 mg), and dry 1,4-dioxane (50 mL) in the nitrogen atmosphere. The mixture was degassed with nitrogen gas (N_2) for 30 minutes, and then copper iodide (25 mg) and $Pd(PPh_3)_2Cl_2$ (10%) catalyst were added. The reaction mixture was refluxed overnight at 100 ^oC, and the completion of the reaction was confirmed by TLC. The solvent was removed by rotary evaporation washed with water and brine solution and extracted in DCM dried over anhydrous sodium sulfate. After evaporation of the solvent, the resultant mixture was purified by column chromatography technique with DCM and hexane (4:1) as eluents, to afford the compound **V** yield (42%). Analytical data

Synthesis of VI: We have adopted a similar reaction procedure to compound **V**, but only the difference is that instead of compound **IV**, we have taken compound **V**. Yield 60%. **MALDI-TOF**: m/z: Calcd for $C_{97}H_{111}N_5O_5S_3Zn$: 1585.70 $[M+H]^+$, Found: 1588.52 $[M+H]^+$.

Synthesis of SPS-PPY-C_{60}: A dry round bottom flask (50 mL) was charged with compound **VI** (100 mg, 0.09 mmol), C_{60} (0.05 g, 0.06 mmol), and N-methylglycine (0.04 g, 0.5 mmol) in toluene (25 mL) and refluxed for 48 h. The reaction solvent was removed by rotary evaporation, washed with water and NaCl solution,and extracted in DCM over anhydrous Na_2SO_4. The organic solvent was removed by rotary evaporation, the crude material was purified by \column chromatography using DCM and hexane (4:1) as eluent, to afford the **SPS-PPY-C_{60}.** Yield = 71%.**^{1}H NMR (300 MHz, $CDCl_3$)** δ 9.59 (dd, *J* = 17.8, 4.4 Hz, 4H), 8.84 (dd, *J* = 4.4, 2.7 Hz, 4H), 7.71 (d, *J* = 9.8 Hz, 5H), 7.52 (d, *J* = 4.3 Hz, 1H), 7.38 (s, 2H), 7.19 (d, *J* = 5.9 Hz, 2H), 6.96 (dd, *J* = 22.3, 8.6 Hz, 8H), 3.84 (t, *J* = 6.0 Hz, 8H), 2.98 (s, 2H), 1.36 – 1.17 (m, 20H), 1.02 – 0.72 (m, 30H), 0.58 (s, 10H), 0.49 (d, *J* = 7.1 Hz, 15H).MALDI-TOF MS Calcd. m/z ($C_{139}H_{125}N_6O_4S_3Zn$) 2105.820, Found 2016.782.

Methods: Details are explained in supporting information.

Results and Discussion

Optical and Electrochemical properties

The optical absorption spectral data of **SPS-PPY-C_{60}** in dichloromethane (DCM) at room temperature along with the control compounds C_{60} and phenothiazine and the respective absorption maxima along with logarithmic molar extinction coefficients are given in Table 1.

The absorption spectrum of **SPS-PPY-C$_{60}$** shown in Figure 1 suggests that both the Soret and Q bands are red-shifted when compared to its control compound tetraphenyl zinc porphyrin (ZnTTP) due to the presence of two ethynyl bridges carrying substituents. An additional peak at ~325 nm is due to the fullerene and phenothiazine moiety was also observed. The molar extinction coefficients of **SPS-PPY-C$_{60}$** were appreciably altered when compared to its control compounds suggesting electronic perturbation due to the ethynyl bridges carrying different donor and acceptor entities.

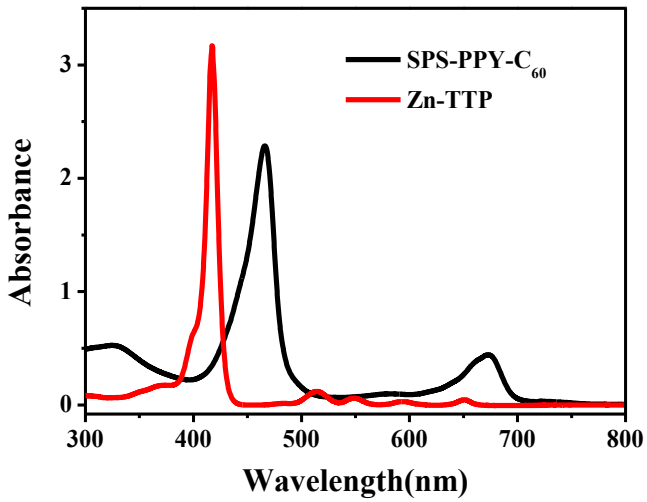

Figure 1. Absorption spectrum of **SPS-PPY-C$_{60}$** and ZnTPP in dichloromethane at room temperature.

Next, the redox properties of **SPS-PPY-C$_{60}$** along with control compounds phenothiazine, ZnTPP, and C_{60} were investigated using differential pulse voltammetry (DPV) technique in *o*-dichlorobenzene containing 0.1 M tetrabutylammonium perchlorate as the supporting electrolyte to evaluate the potentials of different redox states. Figure 2 illustrates the DPVs of **SPS-PPY-C$_{60}$** and respective redox potential data are presented in Table 1. Under the experimental conditions, phenothiazine did not show any reduction process. The **SPS-PPY-C$_{60}$** revealed reversible to quasi-reversible, three to four oxidations and four reductions, under the experimental conditions. The first oxidation was located at 0.77 V vs. Ag/AgCl belonging to the phenothiazine-porphyrin while the second oxidation was at 0.94 V for the porphyrin π-system. Similarly, the first

reduction at -0.54 V belongs to the acceptor fullerene and the remaining reductions belong to the porphyrin and fullerene moieties of **SPS-PPY-C$_{60}$** as individual or overlapped peaks.

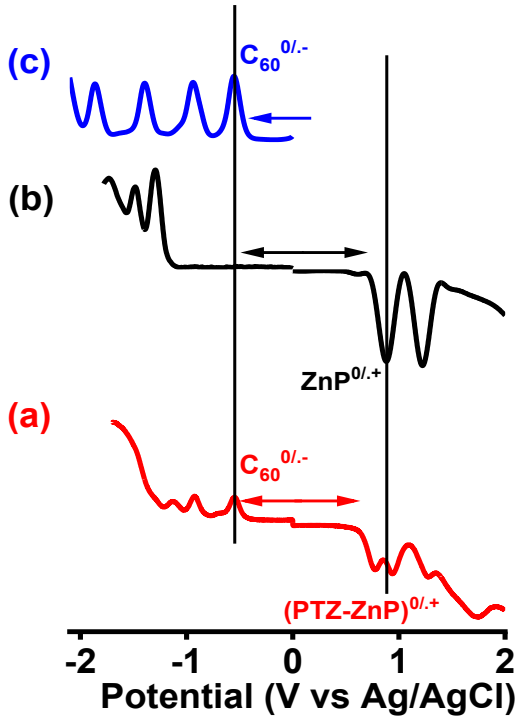

Figure 2. Differential pulse voltammetry of (a) **SPS-PPY-C$_{60}$**, (b) Zn-TTP,and (c) C_{60}in dichloromethane containing 0.1 M $(n\text{-}C_4H_9)_4NClO_4$, with the concentrations of the compounds held ~ 1 mM; scan rate = 10 mV s^{-1}.

Table 1. Optical and redox potential data.

Compound	**Absorption, λ_{max}, nm (log ε, M^{-1} cm^{-1})[a]**	**Potential V vs.AgAgCl[b]** **Reduction**	**Oxidation**
Phenothiazine	254 (4.77)	---	0.59 1.22
C_{60}	256327 (4.76) (3.62)	-0.55 -0.93 -1.40 -1.85	---
ZnTTP	421 552 602 (5.39) (4.57) (3.90)	-1.28 -1.47	0.88 1.22
SPS-PPY-C$_{60}$	260 327 466 673 (4.78) (3.72) (5.42) (4.27)	-0.54 -0.92 -1.12	0.77 0.94 1.27 1.72

[a]Solvent CH_2Cl_2. Error limits λ_{max}, ±1 nm; log ε, ±10%. [b]DCB, 0.1 M TBAP. Platinum working electrode; Ag/AgCl electrode is the reference electrode; Pt electrode is the auxiliary electrode. Error limits, $E_{1/2}$ ± 0.03 V.

Geometry optimization and energy levels

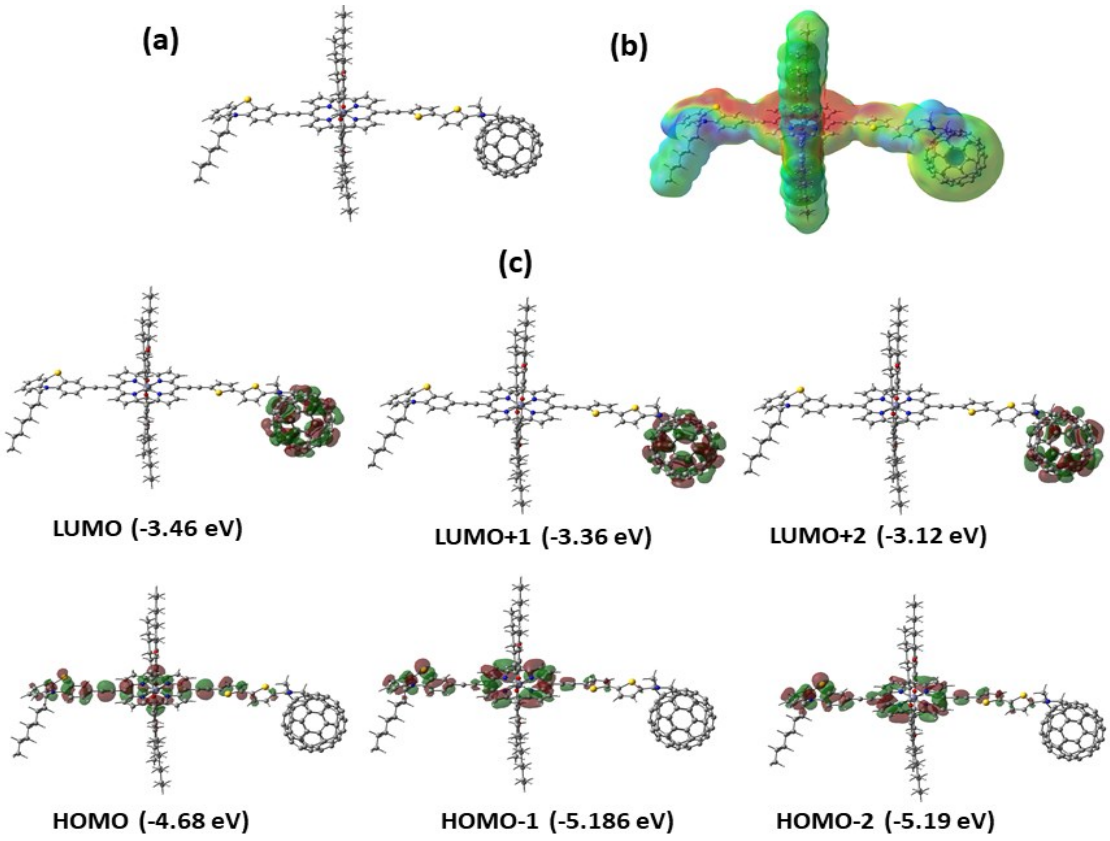

Figure 3. B3LYP/6-311G(d,p)-calculated a) optimized structure, b) electrostatic potential surface: Red=electron rich regions ($-2.000x10^{-2}$ V- $2.000x10^{-2}$), c) frontier LUMO, and frontier HOMO of **SPS-PPY-C_{60}**.

DFT and TD-DFT calculations with a functional basis set of *B3LYP/6-311G(d,p)*level[36,37] to evaluate its structural, optical, and electronic properties were subsequently performed. Ground state optimized geometries of the **SPS-PPY-C_{60}** molecule illustrated in Figure 3a comprises phenothiazine-porphyrin linked by an ethynyl bridge. Whereas the acceptor fullerene is separated by a thiophene that tethered to porphyrin through an ethynyl bridge. Figure 3b demonstrates the molecular electrostatic potential (MEP) maps of **SPS-PPY-C_{60}** revealing the existence of positive electrostatic potential at the phenothiazine-porphyrin, and negative potential generated on the fullerene acceptor group. This suggests that the electron transfer from phenothiazine-zinc

porphyrin to acceptor fullerene. Figure 3c enlightens frontier molecular orbitals (FMOs) of **SPS-PPY-C$_{60}$** in which the electron density distribution of the highest occupied molecular orbital (HOMO) is distributed on the phenothiazine-porphyrin π-plane. This was also the case for the HOMO-1 and HOMO-2, wherein the HOMOs were located on the phenothiazine-porphyrin unit. In contrast, the electron density distribution of the lowest occupied molecular orbital (LUMO) and LUMO+1 and LUMO+2 were on acceptor fullerene exclusively. The gas phase HOMO-LUMO gap of **SPS-PPY-C$_{60}$** was found to be 1.22 eV. In addition, TD-DFT studies on **SPS-PPY-C$_{60}$** system were carried out at the B3LYP/6-311G(d,p) level to understand the excited-state transitions. The calculated vertical excitation energies for singlet together with calculated oscillator strengths are listed in Table S1.

To witness the charge transfer, after optimization of the structure, the ground state charge density was computed and saved, and then for each excited state, the charge density was calculated. Upon completion, the ground state density, the density cube for the excited state of interest, and the subtraction of the two cubes were loaded on the *GaussView 6* program. After subtraction, the remaining density is treated as the difference between the ground state density and the excited state density and is referred to as "charge transfer".

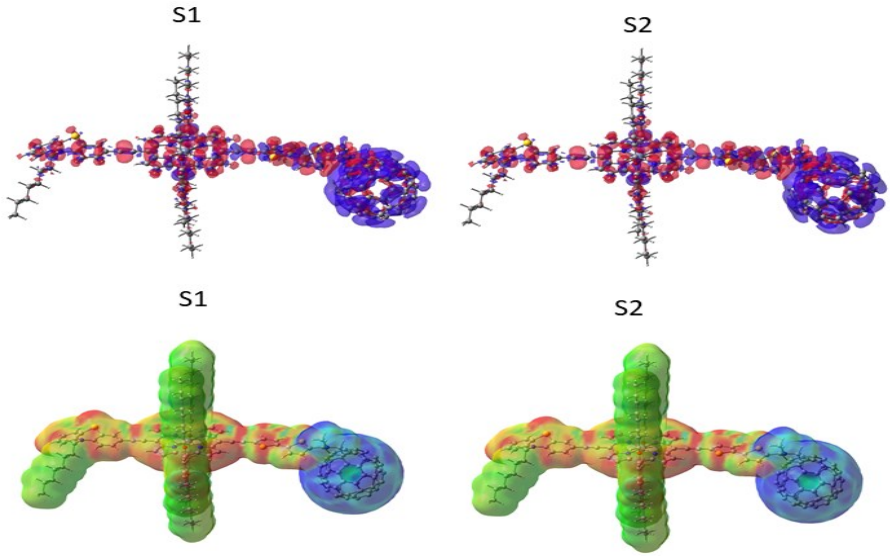

Figure4. Electrostatic potential surfaces (red: charge donor, blue: charge acceptor; -2.000x10^{-5} V – 2.000x10^{-5} V) and the electron density location of charge transfer for the first two excited states of **SPS-PPY-C$_{60}$** on B3LYP/6-311G(d,p) optimized structures.

Figure 4 shows the results of this study, both the electrostatic potential surface and the location of charge transfer in the donor and acceptor parts of **SPS-PPY-C$_{60}$** are exhibited. This computational study confirms the occurrence of charge transfer involving both the S_1 and S_2 states in **SPS-PPY-C$_{60}$** with the phenothiazine-porphyrin unit acting as an electron donor and fullerene as an electron acceptor.[38]

Excited state properties

Unlike the case with the groundstate properties described above, major differences were noticed between the singlet excited state activities of **SPS-PPY-C$_{60}$** and their corresponding constituent units. Figure 5 illustrates the steady-state emission spectra of **SPS-PPY-C$_{60}$** along with its constituent individual i.e., ZnTTP in all three investigated solvents. The emission spectrum of **SPS-PPY-C$_{60}$** was found to be quenched when excited either at 300 nm where phenothiazine absorbs or at 460 nm where porphyrin absorbs majorly in comparison with the control compounds phenothiazine or ZnTTP, respectively. The quenching of emission is possible due to photoinduced electron transfer (PET) or excitation energy transfer (EET).[31]

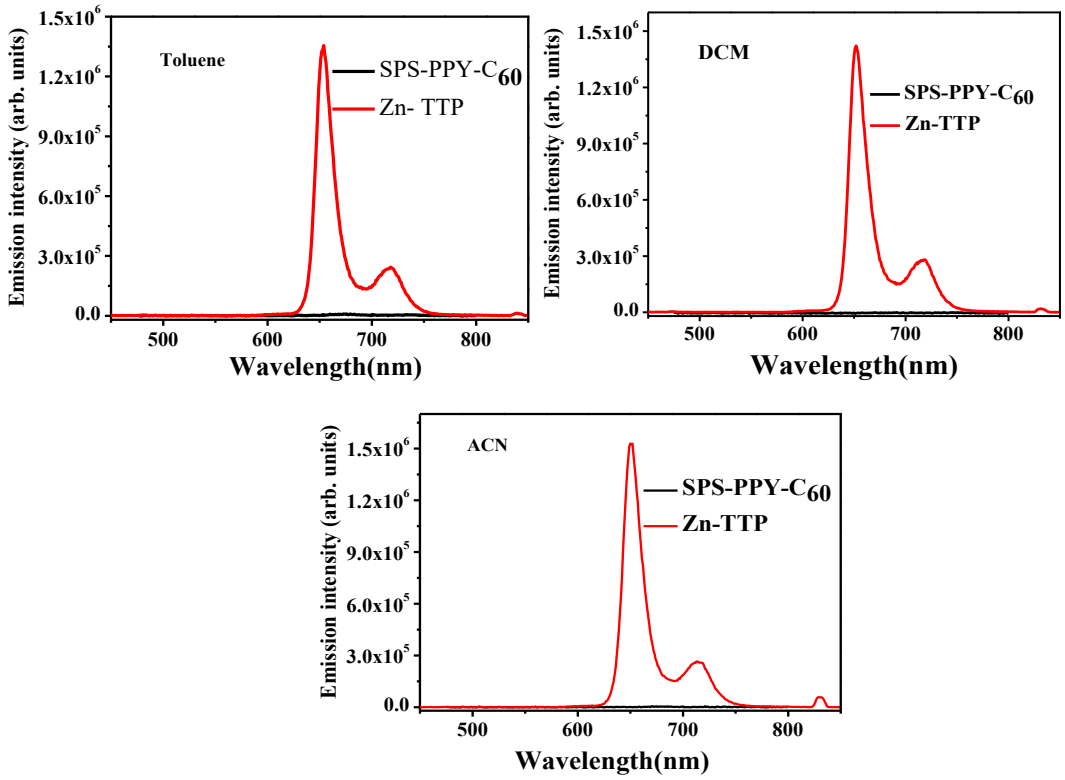

Figure 5. Emission spectrum of **SPS-PPY-C60** and ZnTTP in the indicated solvents, λ_{ex}= 460 nm.

The E_{0-0} (0−0 spectroscopic transition energy) values of the porphyrin part of **SPS-PPY-C60** were found to be 1.86 eV as shown in Figure 6, which is lower than the ZnTTP (2.05 eV), estimated from the intersecting point of excitation and emission spectra. The change in Gibbs free-energy for PET from the phenothiazine-porphyrin to the fullerene can be calculated by using equations i-iii. [39]

$$-\Delta G_{CR} = E_{ox} - E_{red} + \Delta Gs \quad \text{(i)}$$

$$-\Delta G_{CS} = \Delta E_{00} - (-\Delta G_{CR}) \quad \text{(ii)}$$

$$\Delta G_S = \frac{e^2}{4\pi\varepsilon_0}\left[\left(\frac{1}{2R^+} + \frac{1}{2R^-}\right)\Delta\left(\frac{1}{\varepsilon_R}\right) - \frac{1}{R_{CC}\varepsilon_R}\right] \quad \text{(iii)}$$

Where ΔE_{00} denotes the singly excited state energy for the **SPS-PPY-C60**. The first oxidation and first reduction potentials are denoted by the terms E_{ox} and E_{red}, respectively. ΔGs refers to electrostatic energy calculated according to the dielectric continuum model (by using eq iii). The dielectric constant of utilized solvent in photochemical and electrochemical studies and permittivity of vacuum are represented by the symbols, ε_R and ε_0, respectively. The symbols R_+ and R_- represent the radii of the cation and anion, respectively. R_{cc} denotes the center-to-center distance between donor and acceptor parts of the synthesized dyad from the computed structures as shown in Figure 3.

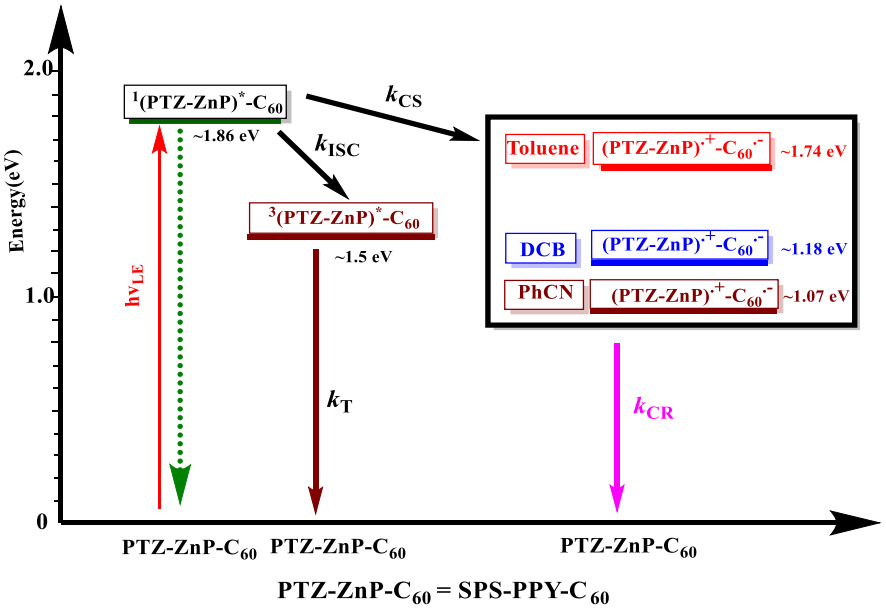

Figure 6. Jablonski-type energy level diagram for the **SPS-PPY-C$_{60}$** push-pull system in studied solvents. Abbreviations: CS = charge separation, CT = charge transfer, CR = charge recombination, ISC = intersystem crossing, F = fluorescence emission, T = triplet emission.

Based on such calculations, an energy profile diagram was constructed as shown in Figure 6. The negative values of change in Gibbs free energy indicate the possibility of PET from phenothiazine-zinc porphyrin to C_{60} in all studied solvents including very low polar toluene. In addition to this, EET from the singlet excited phenothiazine-zinc porphyrin (ΔE_{00} =1.86 eV) to C_{60} (ΔE_{00} =1.75 eV) is also a possibility.

Fluorescence quantum yields of **SPS-PPY-C$_{60}$** were estimated by comparing the emission curves of the reference compound (ZnTTP, ϕ =0.036 ± 0.001, respectively, in CH_2Cl_2 solvent) with that of **SPS-PPY-C$_{60}$**. The quenching efficiency (Q) can be estimated by using equation (iv).

$$Q = \frac{\phi(Zn-TTP) - \phi[\text{SPS - PPY - C}_{60}]}{\phi(Zn-TTP)} \qquad \text{(iv)}$$

where ϕ(ZnTPP) and ϕ(SPS-PPY-C$_{60}$) refer tothe fluorescence quantum yields of ZnTTPand the **SPS-PPY-C$_{60}$**,respectively; (λ_{ex}= 460 nm). The emission quenching efficiency was over 99% in both non-polar and polar solvents which suggests very efficient excited-state events. To secure spectral evidence for the quenching mechanism and kinetic information, femtosecond transient absorption studies were systematically performed as discussed below.

Transient Absorption Studies:

In the end, pump-probe experiments were performed to identify the occurrence of charge separation in **SPS-PPY-C$_{60}$** in solvents of varying polarities. The resulting fs-TA spectra are shown in Figure 7 after exciting at 466 corresponding to the Soret band and in Figure 8 after exciting at 677 nm corresponding to the Q-band at indicated delay times. The transient features in polar benzonitrile and moderate polar dichlorobenzene exhibited very similar characteristics. The instantaneously formed $^1ZnP^*$ revealed excited state absorption bands at 510, 513, 785, 1005, and 1160 nm. The peak at 513 nm could be assigned to the instant formation of $^1ZnP^*$ and its subsequent diminishing producing a long-lived triplet state at 510 nm due to the formation of $^3ZnP^*$. The peak at 785 nm could be assigned to the cationic species by comparing this spectrum

with the spectrum of the **SPS-PPY-C_{60}** cation produced by chemical oxidation (as depicted in Fig. S10). A close examination of the NIR region shows a peak at 1010 nm that could be attributed to $C_{60}^{\cdot-}$ formed during the charge separation process after exciting at 466 nm. Additionally, two negative peaks were observed at 466, and 678 nm could be attributed to ground-state bleaching (GSB) compared with ground-state absorption. Further data was analyzed by GloTarAn[40] and the best results were obtained after providing a four-component fit, representing $S_0 \rightarrow S_1^*(hot) \rightarrow S_1 \rightarrow CS \rightarrow T_1$. The species-associated spectra (SAS) are shown in Figure 7. Time constants were found to be 2 ps for hot S_1^*, 25 ps for S_1, 169 ps for CS, and >3 ns for T_1 in benzonitrile (Figure 7g) whereas in the case of dichlorobenzene (Figure 7h), they were found to be 0.7 ps for S_1^*, 27 ps for S_1, 319 ps for CS, and >3 ns for T_1. Almost similar lifetime values were found for the visible region which are shown in Figures 7d, 7e, and 7f.

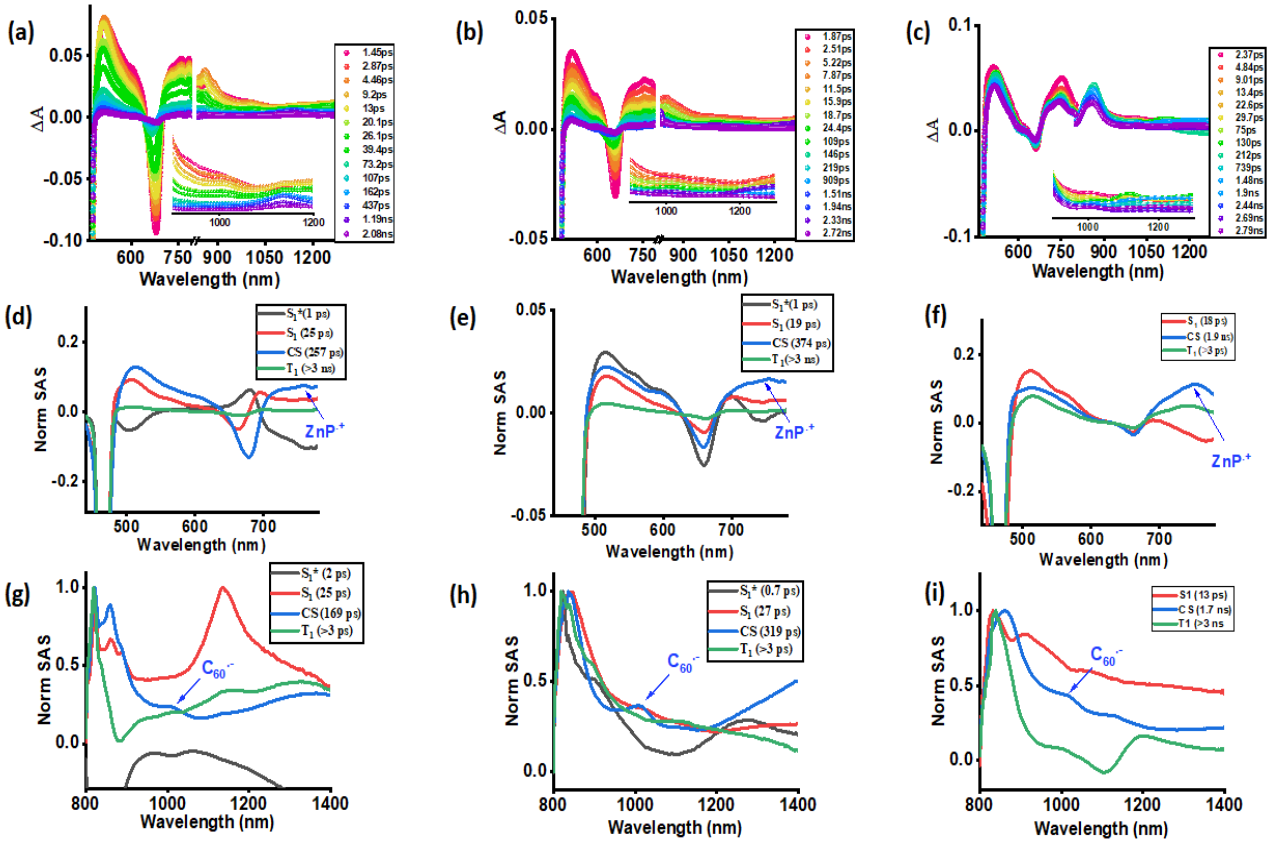

Figure 7. Fs-TA spectrafor **SPS-PPY-C_{60}** in (a) benzonitrile, (b) dichlorobenzene, and (c) toluene after exiting at 466 nm at different delay times. The species-associated spectra for the visible (d-f) and near-IR (g-h) from glotaran analysis are also shown.

In the case of nonpolar toluene, the spectral features were also supportive of charge transfer in support of the energy profile diagram (Figure 6), as shown in Figure 7c. The instantaneously formed $^{1}ZnP^{*}$ revealed excited state absorption bands at 510, 515, 750, 861, and 1020 nm. The peak at 510 nm could be assigned to the instant formation of $^{1}ZnP^{*}$ and its subsequent decay producing a long-lived triplet state at 515 nm associated with the formation of $^{3}ZnP^{*}$. Additionally, two negative peaks were observed at 466, and 664 nm that could be attributed to ground state bleaching (GSB) by comparing with ground state absorption. By comparing these spectra with chemical oxidation, the peak at 750 nm could be attributed to cation formation (Fig. S10). A close examination of the NIR region shows a peak at 1020 nm that could be attributed to C_{60}^{-} formed during the charge separation process after exciting at 466 nm. However, as discussed earlier, the 1000 nm region could also be due to $^{1}C_{60}$*,[41,42] an energy transfer product from singlet excited zinc porphyrin to C_{60}. Such a mechanism could be operative, especially in nonpolar toluene where charge separation is not a preferred quenching mechanism. Interestingly, the transient features shown in Figure 7f reveal spectrum characteristics of the phenothiazine-zinc porphyrin radical cation suggesting the 1000 nm peak could have

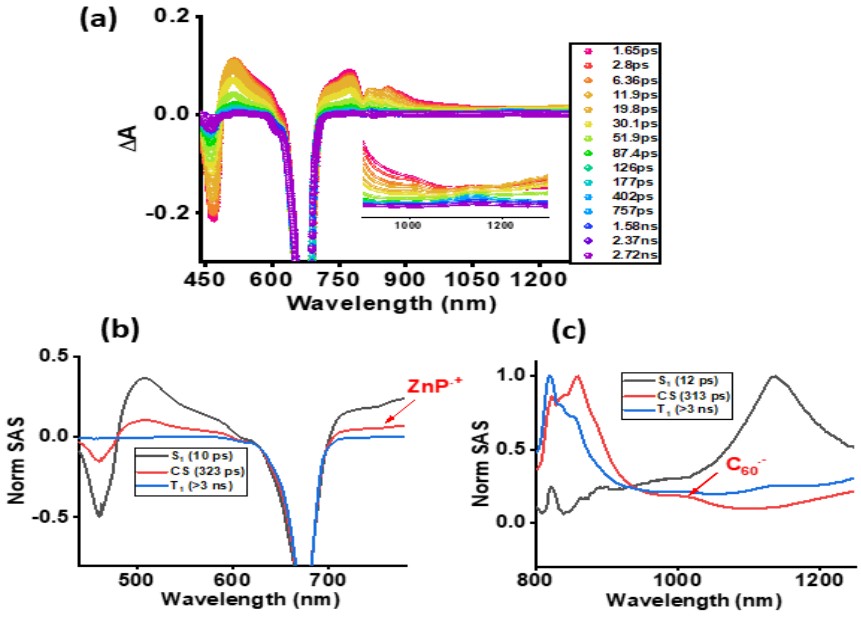

Figure 8. Fs-TA spectra for **SPS-PPY-C$_{60}$** in benzonitrile after exiting at 677 nm at the indicated delay times. The species-associated spectra for the visible (b) and near-IR (c) from glotaran analysis are also shown.

contributions mainly from $C_{60}^{\cdot-}$ and not from $^1C_{60}$*. Further data was analyzed by GloTarAn and the best results were obtained after providing a three-component fit, representing $S_0 \rightarrow S_1 \rightarrow CS \rightarrow T_1$. The species-associated spectra (SAS) are shown in Figure 7i. Time constants were found to be 13 ps for S_1, 1.7 ns for CS, and >3 ns for T_1.

The transient spectra were also recorded by exciting the samples by 677 nm corresponding to the Q-band. Due to the strong light scattered excitation signal and a large signal-to-noise ratio, evidence for charge separation was possible to obtain only in benzonitrile, as shown in Figure 8. From global target analysis, the calculated lifetime of the charge-separated state was ~320 ps.

Conclusions

In summary, the occurrence of excited state charge separation in the newly synthesized **SPS-PPY-C_{60}** in polar to nonpolar solvents has been successfully shown. Ground state absorption of **SPS-PPY-C_{60}** suggested that both Soret and Q-bands of porphyrin moiety are red-shifted due to the π-extended conjugation of two ethyne bridges. Whereas steady state emission spectra when excited at Soret band maxima, revealed quenched emission in all studied solvents that suggested photoinduced electron transfer is taking place in **SPS-PPY-C_{60}**. The redox potential values suggested that both phenothiazine-zinc porphyrin parts of **SPS-PPY-C_{60}** can be easily oxidized which are acting as a donor and the fullerene part is easy to reduce, acting as an acceptor. The redox characteristics were validated by DFT calculation, which showed that the highest occupied molecular orbital (HOMO) is distributed over the phenothiazine-zinc porphyrin entity, and the lowest occupied molecular orbital is spread on the fullerene part. Eventually, femtosecond transient spectroscopic studies were performed to confirm the charge separation. The data was analyzed by GloTarAn and lifetime values for this state were found to be 169 ps in benzonitrile, 319 ps in dichlorobenzene, and 1.7 ns in toluene for Soret band excitation and ~320 ps for Q-band excitation in benzonitrile, was secured. The relatively long lifetime value for the charge-separated state of this investigated compound suggests that it can be used as a model compound for artificial photosynthesis and to construct optoelectronic devices.

Acknowledgments

This work was financially supported by the department of science and technology under the core research grant (DST, CRG/2022/001013 ;GAP-0960) MNR thanks to csir for the senior research fellowship. We thank Director CSIR-IICT for the support (IICT/2024-xxx).

Conflicts of interest

The authors declare no conflicts of interest.

References

1. Sebastiano, C. ; Francesco, N. ; Guiseppina, L. G. ; Scolastica, S. ; Antonio, S. ; Antonio, A. Self-Assembled Systems for Artificial Photosynthesis. *Phys. Chem. Chem. Phys*. **2023**, *25*, 1504-1512.
2. Imahori, H. Molecular Photoinduced Charge Separation:Fundamentals and Applications. *Bull. Chem. Soc., Jpn.* **2023,** *96*, 339−352.
3. Chen, Y. ; Xu, B. ; Yao, R. ; Chen, Ch. ; Zhang, Ch. Mimicking The Oxygen-Evolving Center in Photosynthesis. *Front. Plant Sc*., **2022**, *22*, 929532.
4. Fukuzumi, S. ; Lee, Y. –M. ; Nam, W. Bio-Inspired Artificial Photosynthesis Systems. *Tetrahedron* **2020**, *76*, 131024.
5. Gisriel, C.; Sarrou, I.; Ferlez, B.; Golbeck, J. H.; Redding, K. E.;Fromme, R. Structure of a Symmetric Photosynthetic Reaction Center-Photosystem. *Science* **2017**, *357*, 1021−1025.
6. Giribabu, L. ; Reeta, P. S. ; Kanaparthi, R. K. ; Srikanth, M. ; Soujanya, Y. Bis(Porphyrin)-Anthraquinone Triads : Synthesis, Spectroscopy and Photochemistry. *J. Phys. Chem. A* **2013**, *117*, 2944-2951.
7. Wiehe, A.; Senge, M. O.; Schafer, A.; Speck, M.; Tannert, S.;Kurreck, H.; Roder, B. Electron Donor−Acceptor Compounds:Exploiting the Triptycene Geometry for the Synthesis of Porphyrin Quinone Dyads, Triads, and a Tetrad. *Tetrahedron***2001**, *57*, 10089−10110.
8. Nenavath, S. ; Duvva, N. ; Kaswan, R. R. ; Lim, G. N. ; D'Souza, F. ; Giribabu, L. Intramolecular Photoinduced Energy and Electron Transfer Reactions in Phenanthroimidazole−Boron Dipyromethane Donor−Acceptor Dyads

9. Zarrabi, N.; Holzer, N.; Lim, G. N.; Obondi, C. O.; van der Est, A.; D'Souza, F.; Poddutoori, P. K. Sequential Electron Trasnfer inbis(styryl)BODIPY-Aluminum(III) Porphyrin-Naphthalimide Reaction Center Mimic. *J. Porphyrins Phthalocyanines* 2022, *26*, 407−417.
10. Piradi, V.; Gao, Y.; Yan, F.; Imran, M.; Zhao, J.; Zhu, X.; So, S. K.Thiophene–Perylenediimide Bridged Dimeric Porphyrin Donors Based on the Donor–Acceptor–Donor Structure for Organic Photovoltaics. *ACS Appl. Energy Mater*. **2022**, *5*, 7287-7296.
11. Maity, A.; Ghosh, U.; Giri, D.; Mukherjee, D.; Maiti, T. K.;Patra, S. K. A Water-Soluble BODIPY based 'OFF/ON' FluorescentProbe for the Detection of Cd2+ Ions with High Selectivity and Sensitivity. *Dalton Trans.* **2019**, *48*, 2108−2117.
12. Grover, N.; Chaudhri, N.; Sankar, M. *β*-Substituted Donor-Acceptor Porphyrins: Synthesis, Energy Transfer and Electrochemical Redox Properties. *Dyes Pigments***2019**, *161*, 104-112.
13. Das, S.; Bhat, H. R.; Balsukuri, Jha, P. C.; Hisamune, Y.; Ishida, M.; Furuta, H.; Mori, S.; Gupta, I. Donor–Acceptor Type A_2B_2 Porphyrins: Synthesis, Energy Transfer, Computational and Electrochemical Studies. *Inorg. Chem. Front*. **2017**, *4*, 618-638.
14. Mahmood, A. ; Hu, J. –Y. ; Xiao, B. ; Tang, A. ; Wang, X. ; Zhou, E. Recent Progress in Porphyrin-Based Materials for Organic Solar Cells. *J. Mater. Chem. A* **2018**, *6*, 16769-16797.
15. Yahagh, A.; Kaswan, R. R.; Kazemi, S.; Karr, P. A. ; D'Souza, F. Symmetry Breaking Charge Transfer Leading to Charge Separation in a Far-Red Absorbing Bisstyryl-BODIPY Dimer. *Chem. Sci*, **2024**, *15*, 906–913.
16. Krishna, N. V. ; Krishna, J. V. S. ; Mrinalini, M. ; Prasanthkumar, S. ; Giribabu, L. Role of Co-Sensitizers in Dye-Sensitized Solar Cells.
17. Borges-Martinez, M. ; Montenegro-Pohlhammer, N. ; Yamamoto, Y. ; Baruah, T. ; Cardenas-Jiron, G. Zn(II)-Porphyrin–Squaraine Dyads as Potential Components for Dye-Sensitized Solar Cells: A Quantum Chemical Study of Optical and Charge Transport Properties. *J. Phys. Chem. C***2020**, *124*, 12968-12981.
18. Sokkalingam, P.; Santra, S.; Mangalampalli, R. Synthesis and Photophysical Studies of Non-Covalently Linked Porphyrin Dyads and Triads. *J. Porphyrin Phthalocyanines* **2007**, *11*, 85-94.

19. Kesti, T. J. ; Tkchencko, N. V. ; Vehmanen, V. ; Yamada, H. ; Imahori, H. ; Fukuzumi, S. ; Lemmetyinen, H. Exciplex Intermediates in Photoinduced Electron Transfer of Porphyrin-Fullerene Dyads. *J. Am. Chem. Soc*., **2002**, *124*, 8067-8077.
20. D'Souza, F.; Gadde, S.; Zandler, M. E.; Arkady, K.; El-Khouly, M. E.; Fujitsjuka, M.; Ito, O. Studies on Covalently Linked Porphyrin−C_{60} Dyads: Stabilization of Charge-Separated States by Axial Coordination. *J. Phys. Chem. A* **2002**, *106*, 12393-12404.
21. Cai, B. ; Song, H. ; Brnovic, A. ; Pavliuk, M. V. ; Hammarstrom, L. ; Tian, H.Promoted Charge Separation and Long-Lived Charge-Separated State in Porphyrin-Viologen Dyad Nanoparticles, *J. Am. Chem. Soc*., **2023**, doi.org/10.1021/jacs.3c04372
22. Washburn, S.; Kaswan, R. R.; Shaikh, S, ; Moss, A, ; D'Souza, F, ; Wang, H. Excited-State Charge Transfer in Push–Pull Platinum (II) π-Extended Porphyrins Fused with Pentacenequinone. *J. Phys. Chem. A*, **2023**, *127*, 9040−9051.
23. Moss, A. ; Jang, Y. ; Arvidson, J. ; Want, H. ; D'Souza, F. Highly Coupled Heterobicycle-Fused Porphyrin Dimers: Excitonic Coupling and Charge Separation with Coordinated Fullerene, C_{60}. *Chem. Sus. Chem*. **2023**, *16*, e202202289.
24. Moss, A.; Jang, Y.; Arvidson, J.; Nesterov, V. N.; D'Souza, F.; Wang, H. Aromatic Heterobicycle-Fused Porphyrins: Impact on Aromaticity and Excited State Electron Transfer Leading to Long-Lived Charge Separation. *Chem. Sci*., **2022**, *13*, 9880-9890.
25. Biswas, Ch.; Palivela, S. G.; Giribabu, L.; Soma, V. R.; Raavi, S. S. K. Femtosecond Excited-State Dynamics and Ultrafast Nonlinear Optical Investigations of Ethynylthiophene Functionalized Porphyrin. *Opt. Mater*. **2022**, *127*, 112232.
26. Krishna, N. V.; Krishna, J. V. S. Singh, S. P.; Giribabu, L.; Han, L.; Bedja, I.; Gupta, R. K.; Islam, A. Donor-π−Acceptor Based Stable Porphyrin Sensitizers for Dye-Sensitized Solar Cells: Effect of π-Conjugated Spacers. *J. Phys. Chem. C* **2017**, *121*, 6464-6477.
27. Kelber, J. B.; Panjwani, N. A.; Wu, D.; Gomez-Bombarelli, R.; Lovett, B. W.; Morton, J. J. L.; Anderson, H. L. Synthesis and Investigation of Donor–Porphyrin–Acceptor Triads with Long-Lived Photo-Induced Charge-Separate States. *Chem. Sci.,* **2015**, *6*, 6468-6481.
28. Pleuz, L. L.; Pellegrin, Y.; Blart, E.; Odobel, F.; Harriman, A. Long-Lived, Charge-Shift States in Heterometallic, Porphyrin-Based Dendrimers Formed via Click Chemistry. *J. Phys. Chem. A.* **2011**, *115*, 5069-5080.

29. Xiao, S.; Li, Y.; Li, Y.; Zhuang, J.; Wang, N.; Liu, H.; Ning, B.; Liu, Y.; Lu, F.; Fan, L.; Yang, Ch. Li, Y. Zhu, D. **[**60]Fullerene-Based Molecular Triads with Expanded Absorptions in the Visible Region: Synthesis and Photovoltaic Properties. *J. Phys. Chem. C.* **2004**, *108*, 16677-16685.

30. Reddy, G.; Katakam, R. ; Devulapally, K. ; Jones, L. A. ; Gaspera, E. D. ; Updyaya, H. M. ; Islavath, N. ; Giribabu, L. Ambient Stable, Hydrophobic, ElectricallyConductive Porphyrin Hole-Extracting Materialsfor Printable Perovskite Solar Cells. *J. Mater. Chem. C* **2019**, *7*, 4072-4078.

31. Naresh, D. ; Kolanu, S. ; Deepak, B. ; Raghu, Ch. ; Giribabu, L. ; Spacer Controlled Photo-Induced Intramolecular Electron Transfer in a Series of Phenothiazine-Boron Dipyrromethene Donor–Acceptor Dyads. *J. Photochem. Photobiol. A Chem*. **2015**, *312*, 8-19.

32. D'Souza, F. ; Raghu, Ch. ; Kei, O. ; Mariusz T. ; Navneetha, K. S. ; Melvin, E. Z. ; Maciek, K. R. ; Daniel, T. G. ; Fukuzumi, S. Corrole−Fullerene Dyads: Formation of Long-Lived Charge-Separated States in Nonpolar Solvents. *J. Am. Chem. Soc*., **2008**, *130*, 14263-14272.

33. Thomas, K. T. ; Manapurathu, V. G. ; Prasanth, V. K. Photoinduced Electron-Transfer Processes in Fullerene-Based Donor–Acceptor Systems. *Helvicta Chimica Acta* **2005,** *88*, 1291-1308.

34. Deepak, B. ; Naresh, D. ; Aniban, B. ; Pooja, Sapna, G. ; Ravinder, P. ; Singh, S. P. ; Garg, A. ; Giribabu, L. ; Raghu, Ch. Phenothiazine Functionalized Fulleropyrrolidines: Synthesis, Charge Transport and Applications to Organic Solar Cells. *Photochem. Photobiol. Sci.*, **2022**, *22*, 379-393.

35. Maggini, M.; Scorrano, G.; Prato, M. Addition of Azomethineylides to C_{60}: Synthesis, Characterization, and Functionalization of Fullerene Pyrrolidines. *J. Am. Chem. Soc,* **1993**, *115*, 9798–9799.

36. Becke, D. Density Functional Thermochemistry. III. The role of Exact Exchange. *J. Chem. Phys*. **1993**, *98*, 5648−5652.

37. Petersson, G. A.; Al-Laham, M. A. A complete Basis set Model Chemistry. II. Open Shell Systems and the Total Energies of the First-Row Atoms. *J. Chem. Phys*. **1991**, *94*, 6081−6090.

38. Ileperuma, C. V.; Garcés-Garcés, J.; Shao, S, ; Fernández-Lázaro, F.; Sastre-Santos, Á.; Karr, P. A.; D'Souza, F. Panchromatic Light-Capturing Bis-styryl BODIPY-Perylenediimide Donor-Acceptor Constructs: Occurrence of Sequential EnergyTransfer Followed by ElectronTransfer. *Chem. Eur. J*, **2023**, 29, e2023016.
39. Rehm, D.; Weller, A. Kinetics of Fluorescence Quenching by Electron and H-Atom Transfer. *Isr. J. Chem*, **1970**, *7*, 259–276.
40. *Glotaran*, http://glotaran.org/
41. Imahori, H. ; Hagiwara, K.; Akiyama, T. ; Aoki, M. ; Taniguchi, S. ; Okada, T. ; Shirakawa, M. ; Sakata, Y. The Small Reorganization Energy of C_{60} in Electron Transfer. *Chemical Physics Letters,* **1996**, *263*, 545-550.
42. Ito, O.; D'Souza, F. Recent Advances in Photoinduced Electron Transfer Processes of Fullerene-Based Molecular Assemblies and Nanocomposites. *Molecules*, **2012**, *17*, 5816-5835.

Table of content